

Cation Distribution and Interatomic Interactions in Oxides with Heterovalent Isomorphism: III.¹ Complex Aluminates LnCaAlO_4 (Ln = Y, La, Nd, Gd, Ho, Er, Yb)

Yu. E. Smirnov and I. A. Zvereva

St. Petersburg State University, St. Petersburg, Russia

Received February 7, 2000

Abstract—The heterovalent isomorphism of Ln^{3+} and Ca^{2+} cations in stoichiometric LnCaAlO_4 oxides was studied. The X-ray diffractometry of the intensity of Laue background modulations revealed a positive short-range ordering in Ln^{3+} and Ca^{2+} distribution over points of one structural site common for both ions, which results in formation of stable $\text{Ln}^{3+}\text{--Ca}^{2+}$ couples in adjacent nine-coordinate oxygen polyhedra. The degree of ordering and the interchange energy estimated in the quasichemical approximation depend both on the effective cationic charges and on the number of unpaired f electrons of the lanthanide atom.

The concentration ranges of isomorphism of differently charged cations in the structures of ionic solid solutions are usually narrow (≤ 0.1 mole fraction). At the same time, in the crystal structures of such complex oxides as $\text{AA}'\text{BO}_4$, $\text{Ad}_2\text{B}'\text{B}_2\text{O}_7$, $\text{A}_3\text{A}'\text{B}_3\text{O}_{10}$, $\text{AA}'\text{B}_2\text{O}_6$, $\text{AA}'\text{O}_4$, etc. (A and A' are isomorphous differently charged cations), there are almost no concentration ranges and the $[\text{A}]/[\text{A}']$ ratios are determined exclusively by the stoichiometry of the compound. In these oxides, like in solid solutions, cations statistically fill equivalent points of one (or more) common structural site. Disordered distribution of isomorphous atoms in a crystal suggests existence of structural heterogeneities of the composition (structural clusters), i.e., local volumes enriched with atoms of the same kind. With differently charged cations A^{+m} and A^{+n} in the absence of compensating vacancies, these clusters can have significant charges. Such reasoning contradicts the equilibrium disordered structural model of oxides. The above statistical structures can be stable only under specific thermodynamic conditions; otherwise, ordering or segregation of isomorphous atoms must take place, resulting either in disintegration of the compound or in changes in its structural state.

Here we present the results of study of the short-range ordering of Ln^{3+} and Ca^{2+} cations in complex aluminates LnCaAlO_4 (Ln = Y, La, Nd, Gd, Ho, Er, Yb), which can efficiently decrease the probability of

appearance of volume charges in the crystal, as well as of interatomic interactions affecting the degree of ordering. For oxides LnCaAlO_4 (Ln = Gd, Ho, Er, Yb) we first determined atomic coordinates and interatomic distances. The oxide YbCaAlO_4 was synthesized for the first time.

Oxides LnCaAlO_4 crystallize in the K_2NiF_4 structural type (space group $I4/mmm$), where Ln and Ca atoms fill with equal probability oxygen nine-vertex polyhedra (single-cap tetragonal distorted antiprisms), and aluminum fills layers of oxygen octahedra (Figs. 1a and 1b). Such crystal structures are described in the literature in three ways:

(1) monolayers of perovskite-like cells shifted relative to each other by half the vector of the diagonal of the square facet of the unit cell base [2];

(2) interpenetrating perovskite (P) and rock salt (RS) structural fragments with alternating layers [...(P)(RS)P(RS)P(RS)...] [3];

(3) alternating atomic nets [...(AlO_2)(AO)(AO)·(AlO_2)(AO)(AO)...] with a well-defined c period of the structure [4] (here and hereinafter, A relates to one of the isomorphous Ln or Ca atoms).

Table 1 lists the results of refinement (in the $I4/mmm$ space group) of the crystal structures of four LnCaAlO_4 oxides by full-profile X-ray patterns. Table 2 gives the interplanar distances and integral intensities for YbCaAlO_4 , which are absent from the PDF data base. Typical experimental and calculated X-ray patterns of YbCaAlO_4 are represented in Fig. 2.

¹ For communication II, see [1].

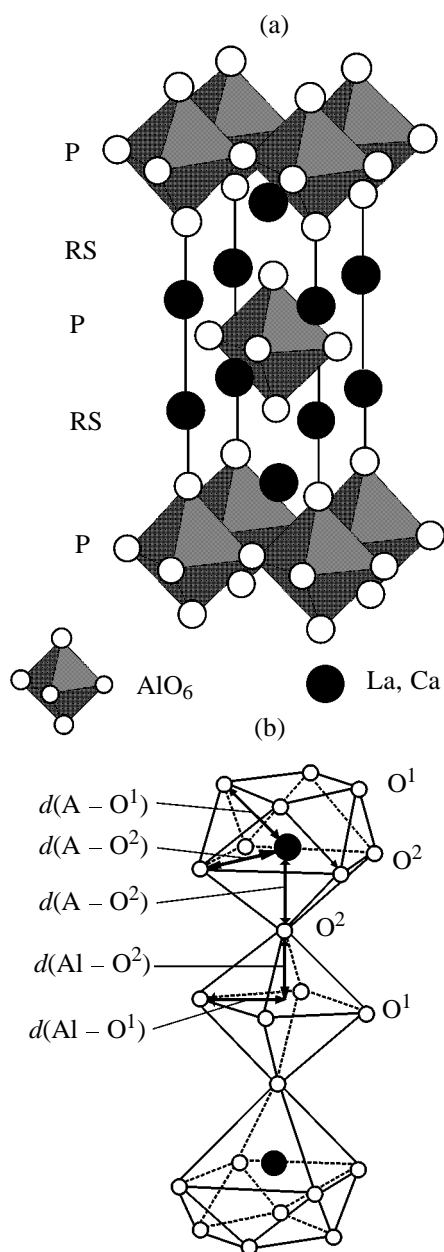


Fig. 1. (a) Unit cell of LnCaAlO_4 and (b) coordination polyhedra AO_9 and AlO_6 .

In going from lanthanum to ytterbium, the unit cell parameters (a , c) and volumes (V) of the oxides generally vary in a fashion expected from the decreasing ionic radii $r(\text{Ln}^{3+})$ of the lanthanide (Table 3). A slightly advanced contraction of the structure along the c axis is only observed, which is attested by the listed $c/3a$ values. Simultaneously, increasing distortion (relative contraction along c) of the perovskite-like cell inside the layer and shortening of the AO^2 bond (characterizing interlayer linking) take place. No pronounced changes in the shift of cations A from oxygen planes (δ) is observed (except for LaCaAlO_4).

Table 1. Atomic coordinates (x , y , z), heat parameters (B), and structural (R_{f}) and profile (R_{p}) divergence factors ($R = \frac{\sum |I_0 - I_c|}{\sum I_0}$) for aluminates LnCaAlO_4

Parameter	GdCaAlO ₄	HoCaAlO ₄	ErCaAlO ₄	YbCaAlO ₄
(Ln,Ca) –				
– 4(e)				
0 0 z	0.3585(1)	0.3581(1)	0.3583(1)	0.35796(8)
B , Å ²	0.34(3)	0.76(4)	0.30(4)	0.23(1)
Al – 2(a)				
0 0 0				
B , Å ²	0.25(11)	0.23(12)	0.41(13)	0.48(2)
O ¹				
0 0.5 0				
B , Å ²	0.9(2)	0.8(2)	0.9(2)	0.89(2)
O ²				
0 0 z	0.1669(7)	0.1682(6)	0.1687(7)	0.1684(5)
B , Å ²	1.0(2)	1.1(2)	1.3(2)	1.31(2)
R_{f} , %	3.57	4.20	3.71	4.03
R_{p} , %	6.75	7.18	6.69	10.99

Table 2. Interplanar distances and calculated integral intensities for polycrystalline YbCaAlO_4 sample in filtered $\text{CuK}\alpha$ radiation as given by full-profile structure refinement (after Rietveld)

d , Å	$h k l$	I_{c} , %	d , Å	$h k l$	I_{c} , %
5.882	0 0 2	<1	1.230	0 1 9	<1
3.478	0 1 1	42	1.207	0 3 1	2
2.941	0 0 4	20	1.179	2 2 4	5
2.668	0 1 3	100	1.177	0 0 10	1
2.574	1 1 0	80	1.169	1 2 7	12
2.358	1 1 2	11	1.159	0 3 3	8
1.976	0 1 5	12	1.151	1 3 0	11
1.961	0 0 6	15	1.144	0 2 8	6
1.937	1 1 4	52	1.130	1 3 2	<1
1.820	0 2 0	44	1.079	0 3 5	1
1.739	0 2 2	<1	1.076	2 2 6	6
1.613	1 2 1	10	1.072	1 3 4	12
1.560	1 1 6	13	1.070	1 1 10	5
1.548	0 2 4	12	1.026	0 1 11	8
1.526	0 1 7	15	1.019	1 2 9	<1
1.504	1 2 3	38	1.006	2 3 1	3
1.471	0 0 8	4	0.9928	1 3 6	7
1.339	1 2 5	6	0.9881	0 2 10	4
1.334	0 2 6	13	0.9839	0 3 7	4
1.287	2 2 0	12	0.9804	0 0 12	0
1.277	1 1 8	5	0.9779	2 3 3	12
1.257	2 2 2	0	0.9686	2 2 8	5

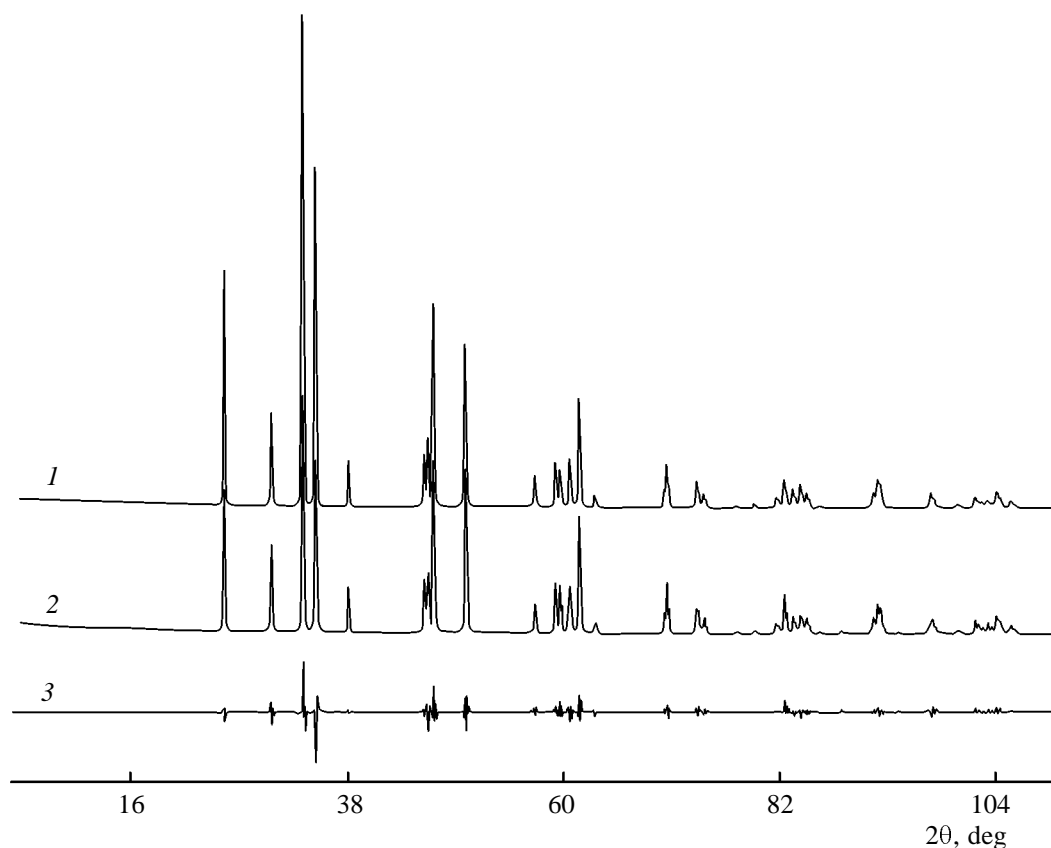


Fig. 2. (1) Calculated, (2) experimental, and (3) difference X-ray diffraction profiles of YbCaAlO_4 in the scattering angle–intensity coordinates.

Table 3. Structural characteristics of LaCaAlO_4 oxides^a

Parameter	YCaAlO_4^b	LaCaAlO_4^c	NdCaAlO_4^b	GdCaAlO_4	HoCaAlO_4	ErCaAlO_4	YbCaAlO_4
a	3.645	3.713	3.685	3.659	3.643	3.640	3.641
c	11.874	12.325	12.124	11.988	11.873	11.838	11.766
$V, \text{\AA}^3$	157.77	169.92	164.61	160.49	157.68	156.87	156.20
$c/3a$	1.086	1.106	1.097	1.092	1.086	1.084	1.077
$r(\text{Ln}^{3+})^d$	1.075	1.216	1.163	1.107	1.072	1.062	1.042
AO_9							
$\text{A}-\text{O}^2 \times 1$	2.260	2.407	2.327	2.296	2.256	2.245	2.228
$\text{A}-\text{O}^1 \times 4$	2.481	2.544	2.518	2.495	2.482	2.475	2.472
$\text{A}-\text{O}^2 \times 4$	2.596	2.640	2.623	2.605	2.595	2.594	2.596
δ/c	0.0261	0.0225	0.0249	0.0254	0.0263	0.0267	0.0264
AlO_6							
$\text{Al}-\text{O}^1 \times 4$	1.823	1.857	1.842	1.829	1.822	1.820	1.821
$\text{Al}-\text{O}^2 \times 2$	1.994	2.031	2.019	2.001	1.997	1.997	1.980
r_1/r_2	0.924	0.937	0.932	0.928	0.925	0.921	0.917

^a Unit cell parameters a and c , interatomic distances in the AO_9 and AlO_6 polyhedra, Ln^{3+} cation radii (\AA), volumes V , $c/3a$ ratios, perovskite-like cell distortion parameters r_1/r_2 , and shifts of isomorphous atoms from oxygen planes δ/c are given.

^b Data of [5]. ^c Data of [6]. ^d Data of [7] for the coordination number 9.

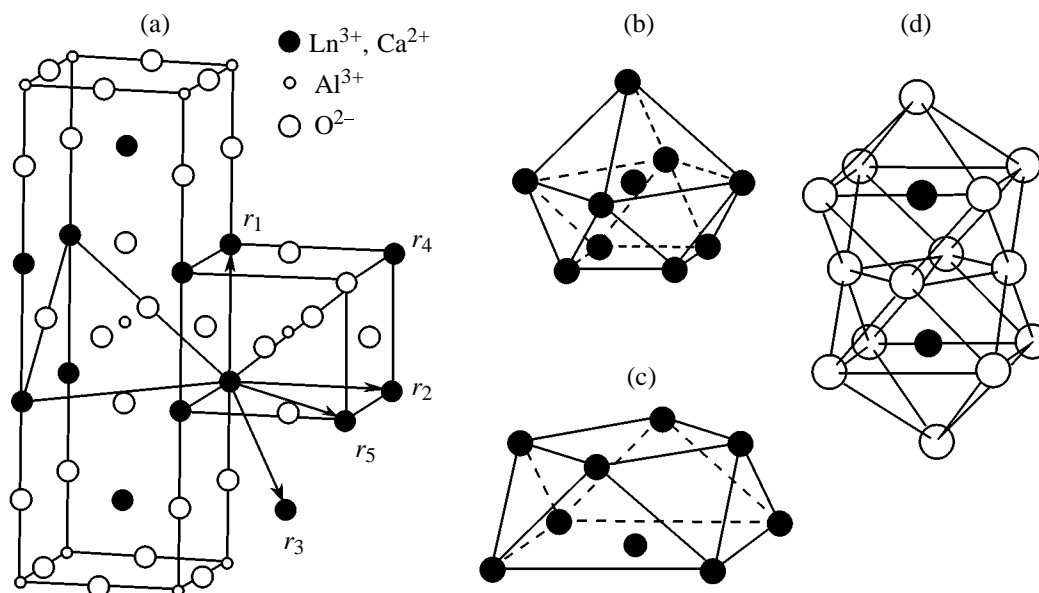


Fig. 3. (a) Unit cell of LaCaAlO₄ with an atomic plane close to (113) and vector radii of the first five cationic coordination spheres; (b, c) the first and second combined cationic coordination spheres; and (d) La³⁺-Ca²⁺ couple in adjacent shared antiprisms.

Table 4. Coordination numbers and radii of cationic coordination spheres for LaCaAlO₄ oxides

Parameter	YCaAlO ₄	LaCaAlO ₄	NdCaAlO ₄	GdCaAlO ₄	HoCaAlO ₄	ErCaAlO ₄	YbCaAlO ₄
1 × r ₁	3.368	3.478	3.434	3.394	3.370	3.354	3.340
4 × r ₂	3.645	3.713	3.685	3.659	3.643	3.640	3.618
4 × r ₃	3.640	3.755	3.701	3.668	3.638	3.633	3.641
9 × R _I	3.612	3.706	3.664	3.634	3.610	3.605	3.597
4 × r ₄	4.963	5.088	5.036	4.990	4.963	4.950	4.944
4 × r ₅	5.155	5.251	5.211	5.174	5.153	5.148	5.150
8 × R _{II}	5.059	5.170	5.124	5.082	5.058	5.049	5.047

The most direct experimental technique for studying short-range ordering is X-ray diffractometry of the intensity of Laue background modulations, i.e., the diffuse scattering beyond Bragg's structural maxima [8]. Earlier it was successfully used for solving similar problems for metal, oxide, and halide substitution solid solutions under the temperature and concentration conditions corresponding to the single-phase region of the phase diagram. With its help we obtained the first data on the ordering of isomorphous cations in stoichiometric LaCaAlO₄ and YCaAlO₄ oxides [6, 9].

Short-range ordering is quantitatively characterized by Cowley's parameters α_i (short-range order coefficients) determined as $\alpha_i = 1 - P_{AB}/C_B$, where P_{AB} is the probability of location of atom B in the i th coordination sphere of atom A, and $C_B = (1 - C_A)$ is the

average concentration of atoms B atoms in a compound or solution. The character or type of the short-range ordering can be judged from the sign of α_i for the first coordination sphere. If $\alpha_1 > 0$, the short-range ordering is said to be negative, i.e., short-range phase separation takes place. If $\alpha_1 < 0$, a positive short-range takes place, when contacts between of unlike atoms are preferable. The parameters α_i commonly fast approach zero as i increases, and thus we can restrict our calculations to several nearest coordination spheres.

The a_i values for LaCaAlO₄ we determined within local volumes containing five first cationic coordination spheres. The corresponding vector radii r_i are shown in Fig. 3a. The lengths of r_i vectors and the coordination numbers are given in Table 4. The r_i values were obtained by full-profile refinement of

oxide crystal structures by Rietveld's method. Since r_1-r_3 and r_4-r_5 are close, a_i were calculated in the approximation of two combined spheres with the averaged radii $R_I = (r_1 + 4r_2 + 4r_3)/9$ and $R_{II} = (r_4 + 4r_5)/8$ and with the coordination numbers 9 and 8. Their coordination polyhedra are shown in Figs. 3b and 3c. Then in the approximation of two coordination spheres and with no regard to the dimensional effect (atomic shifts) [6] the Laue background intensity in the electron units is described by Eq. (1).

$$I_L = NC_{Ln}C_{Ca}(f_{Ln} - f_{Ca})^2 \times \left[1 + 9\alpha_I \frac{\sin(SR_I)}{SR_I} + 8\alpha_{II} \frac{\sin(SR_{II})}{SR_{II}} \right]. \quad (1)$$

Here I_L is the intensity of the Laue background; N is the number of couples of isomorphous Ln and Ca atoms; C_{Ln} , C_{Ca} , f_{Ln} , and f_{Ca} are the concentrations and atomic amplitudes of Ln and Ca; α_I and α_{II} are the short-range ordering coefficients for the first and second combined cationic coordination spheres; $S = 4\pi \sin \tau / \lambda$ is the modulus of the diffraction vector; 2τ is the scattering angle; λ is the wavelength of CuK_α radiation. In the absence of ordering in the arrangement of Ln and Ca atoms, the angular dependence of I_L has the shape of a domed curve $(f_{Ln} - f_{Ca})^2$. In the angle range $9^\circ \leq 2\tau \leq 24^\circ$ this dependence is almost linear. In the presence of positive or negative short-range orderings, the I_L curve begins to oscillate about $(f_{Ln} - f_{Ca})^2$. An example of such oscillation is given in Fig. 4. In Eq. (1), the intrinsic modulation is determined by Eq. (2):

$$\Sigma = 9\alpha_I \frac{\sin(SR_I)}{SR_I} + 8\alpha_{II} \frac{\sin(SR_{II})}{SR_{II}} + D. \quad (2)$$

Here $D = 9\beta_I[\sin(SR_I)/SR_I - \cos SR_I]$ is the parameter of atomic shifts, which is taken into account only for atoms in the first coordination sphere, since even the β_I coefficient is smaller than α_I and α_{II} by a factor of several tens.

The Σ values will oscillate about zero. The dependences of experimental Σ on the scattering angle 2θ are given in Fig. 5 for seven $LnCaAlO_4$ oxides. In all the cases, Σ first increases rather sharply and then either passes a maximum or slows down in its increase. We point out that the intensity of the diffuse scattering is usually smaller than the intensity of Bragg's maxima by two–three orders of magnitude. Hence, the distinct difference in the trends in Σ for the last five samples (obtained by the ceramic procedure) at large scattering angles can be associated with the presence of microadmixture undetectable by X-ray phase analysis. Undoubtedly, this can affect the absolute values of α_I and α_{II} , calculated by minimiz-

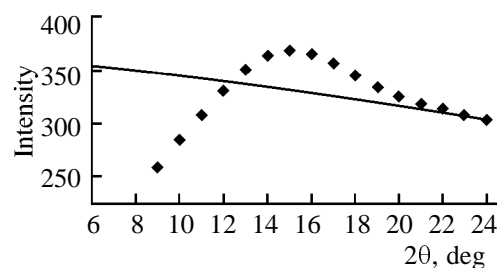


Fig. 4. (points) Modulation of the Laue background intensity I_L about theoretical values of $(f_{Ln} - f_{Ca})^2$ for $YCaAlO_4$.

ing the experimental and calculated Σ values over the entire angular range of measurements. The experience of multiple calculations for repeatedly synthesized $NdCaAlO_4$ samples allowed the error in α_I and α_{II} to be estimated at 30%.

The resulting short-range ordering parameters and rms deviations (σ) of Σ are given in Table 5. The data point to the fact that in all the cases a positive short-range order in arrangement of isomorphous cations takes place, i.e., contacts between different atoms are preferable. The calculated probabilities of such contacts $P_{AB}(R_I)$ exceed the statistical mean value of 0.5. This is the main result of the work, which seems to be natural in our opinion, since any ordering of the differently charged Ln^{3+} and Ca^{2+} cations decreases the probability of formation of structural clusters with volume charges.

The interchange energy (the energy of replacement of one mole of couples of unlike atoms by couples of like atoms), $w = (U_{AA} + U_{BB})k - U_{AB}$ (U_{ij} is the energy of interaction between the i th and j th atoms) was calculated in the quasichemical approximation [8] by Eq. (3). The w values calculated for $1450^\circ C$ are given in Table 5. For all the oxides under study they

Table 5. Short-range order parameters α_i within two combined cation coordination spheres (R_I and R_{II} radii), order energies w , and probabilities P_{AB} for $LaCaAlO_4$ oxides

$LnCaAlO_4$	α_I	α_{II}	σ , %	$P_{AB}(R_I)$	$P_{AB}(r_I)$	w , J/mol
$YCaAlO_4$	-0.071	-0.045	2.6	0.54	0.82	2037
$LaCaAlO_4$	-0.086	+0.003	1.6	0.54	0.89	2470
$NdCaAlO_4$	-0.053	-0.007	2.8	0.53	0.74	1520
$GdCaAlO_4$	-0.041	-0.073	1.1	0.52	0.68	1175
$HoCaAlO_4$	-0.047	-0.047	1.7	0.52	0.71	1348
$ErCaAlO_4$	-0.049	-0.035	1.4	0.52	0.72	1405
$YbCaAlO_4$	-0.056	-0.047	1.4	0.53	0.75	1606

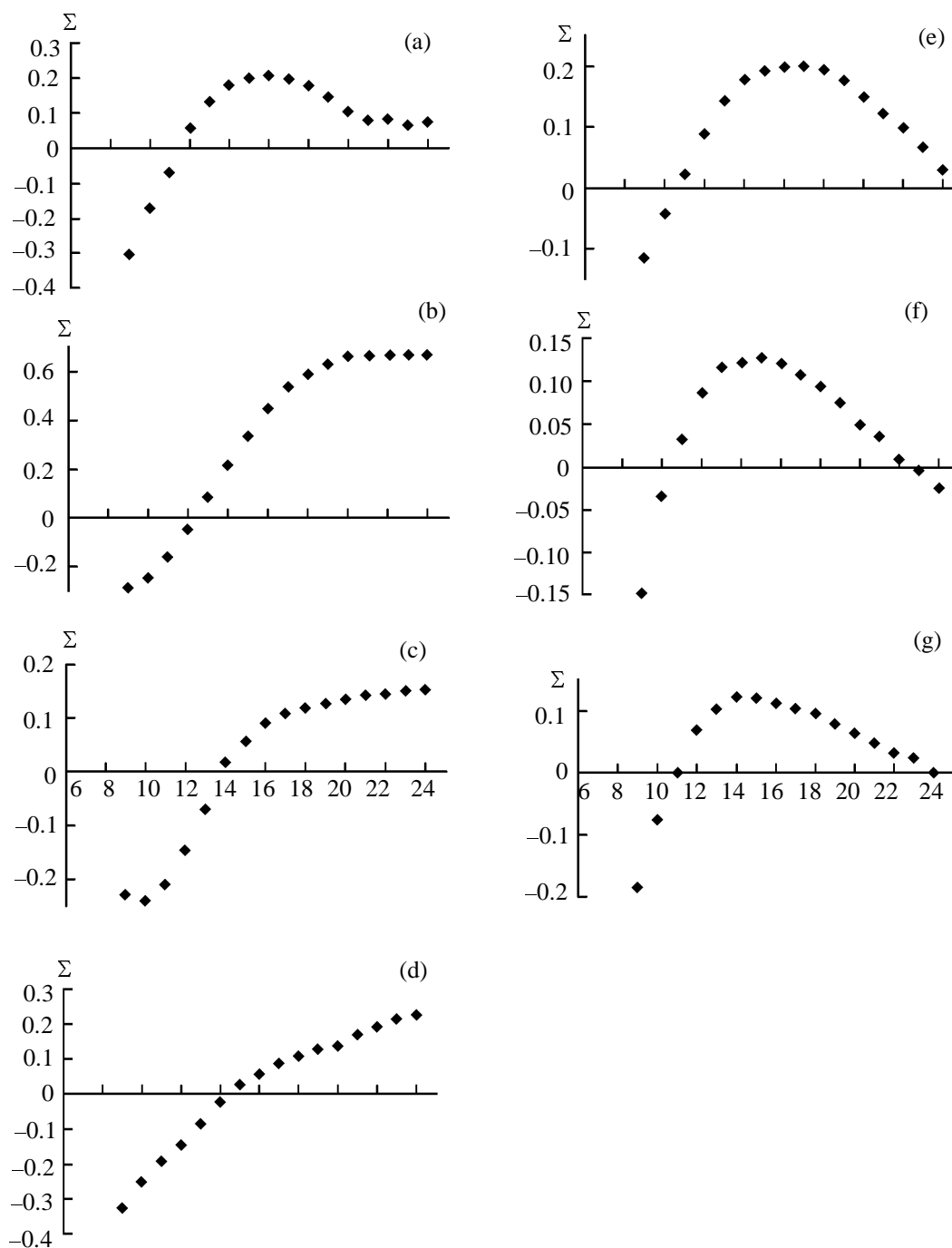


Fig. 5. Modulating component Σ for LnCaAlO_4 oxides at the scattering angles 9–24°. (a) YCaAlO_4 , (b) LaCaAlO_4 , (c) NdCaAlO_4 , (d) GdCaAlO_4 , (e) HoCaAlO_4 , (f) ErCaAlO_4 , and (g) YbCaAlO_4 .

appeared to be of the same order of magnitude as for solid solutions [8].

On the assumption that the main driving force of ordering consists in electrostatic interactions, which are the most efficient at the shortest distances r_1 , we can estimate the probability of formation of a linked $\text{Ln}^{+3}\text{--Ca}^{+2}$ cation couple located in the neighboring

oxygen antiprisms along the c axis and shared, as is seen in Fig. 3d, by a common square base $P_{\text{AB}}(r_1)$. The numerical values of this probability (Table 5), too, essentially differ from the statistical mean value of 0.5. For LaCaAlO_4 the short-range ordering parameter for the second coordination sphere becomes positive, i.e. contacts of like atoms are more probable in the second coordination sphere. This points to the

fact that in this oxide an orientational ordering (antiparallel orientation) of cation couples themselves now takes place inside the layer of perovskite-like cells. That is why, as we reported earlier [10, 11], LaCaAlO_4 stands out of this series of compounds by its thermal instability. In the range 900–1400°C this oxide rather quickly decomposes to related cubic phases of perovskite LaAlO_3 and CaO . The decomposition is a multistage process [9] and begins with enrichment of planes close to $\{113\}$ in lanthanum atoms. One of such planes is shown in Fig. 3a.

The α_1 values for oxides with diamagnetic cations (Y, La) are larger in absolute value than those for oxides with paramagnetic cations. The minimal degree of ordering, i.e. the greatest number of Ln–Ln couples is observed in GdCaAlO_4 (seven unpaired electrons). We explain this fact by additional interaction between the paramagnetic lanthanide atoms (spin–spin or dipole–dipole magnetic interaction), that competes with the purely electrostatic interaction between calcium and gadolinium atoms through oxygen plane. From this point of view, of interest is the structure of layered NaLnTiO_4 oxides (Ln = Sm, Eu, Gd). Owing to the large difference between the effective charges of Na^+ and Ln^{3+} , Na–Ln couples in these oxides are stabilized to the point that no isomorphism is longer possible: The structural site, which was common in the K_2NiF_4 type, is split into two sites, and the symmetry falls to *Pbcm* [12]. Therewith, the couples appear to be ordered inside the perovskite layer in parallel orientation and in the neighboring layers, in the antiparallel orientation. Such orientation ordering results in that RS layers in NaLnTiO_4 consist exclusively of lattice couples of either NaO or LnO , and the r_2 and r_3 distances in the first combined coordination sphere are characteristic of like cations only.

Further study of the dependence of the short-range ordering on the number of unpaired electrons in Ln^{+3} can be performed by introducing additional paramagnetic atoms of 3d elements into aluminum sites, assuming that stronger *d–f* interactions will stronger affect both structural parameters and the degree of ordering.

It should be noted in conclusion that heterovalent stoichiometric isomorphism is encountered only in compounds with essentially ionic chemical bonds, i.e., in oxides, fluorides, and oxyfluorides, where the energy of interatomic interactions in the crystal structure is most contributed by electrostatic interactions. Hence, the hypothesis on the existence in such compounds of electrostatically bound stable couples of differently charged isomorphous cations, we develo-

ped in [6] and in the present work, seems reasonable and fruitful. This hypothesis explains thermodynamic stability or instability and dielectric properties of individual representatives of the oxide series under consideration. The main conclusion that the statistics in distribution of mixed cation couples over points of one structural site substitutes for the statistics in cation distribution within the same structural type is the refinement of the crystal-chemical model of LnCaAlO_4 oxides.

EXPERIMENTAL

Five complex oxides LaCaAlO_4 were synthesized by the ceramic technique rare-earth metal and aluminum oxides and calcium carbonate taken in ratios corresponding to the reaction $\text{Ln}_2\text{O}_3 + \text{Al}_2\text{O}_3 + 2\text{CaO}_3 = 2\text{LnCaAlO}_4 + 2\text{CO}_2$. A thoroughly mixed batch was pressed into pellets and calcined in a corundum crucible in air for 2 h at 900°C and then for 30 h at 1450°C.

LaCaAlO_4 and YCaAlO_4 were obtained by grinding single crystals grown by the zone melting procedure at the Institute of Silicate Chemistry of the Russian Academy of Sciences.

The chemical composition and the uniformity of element distribution over sample surfaces were proved by the microprobe analysis using a Hitachi-2000 scanning electron microscope.

Phase composition was controlled by X-ray diffraction. The X-ray patterns were taken on Siemens D-500 and Philips Analytical PW-3020 X-ray PW-3020 diffractometers (CuK_α radiation). Phase identification was performed using the DIFFRAC-AT program complex (Version 3.1). The X-ray patterns for structural calculations were recorded in the 2τ range of 5°–110° at 0.04° steps at a constant counting time of 12 s.

The intensities of Laue background were measured in a vacuum chamber on a DRON-1 X-ray diffractometer by the Bragg–Brentano scheme with monochromatization of reflected beam. The intensity of scattered radiation was recorded point by point (scan step 1°) in a narrow angle range ($9^\circ \leq 2\tau \leq 24^\circ$), where structural maxima of noticeable intensity are absent, collecting 3600 pulses in every point. Thus we could neglect thermal diffuse scattering. The experimental scattering intensities were corrected for polarization and Compton scattering. The α_1 and α_{II} values were calculated with and without regard for atomic shifts in the first coordination sphere (dimensional effect). No corrections for double Bragg scattering were introduced.

The unit cell parameters, atomic coordinates, and interatomic distances were calculated and refined in the $I4/mmm$ space group on the basis of full-profile structural analysis (after Rietveld [13]). The calculations were performed using the CSD (Crystal Structure Determination) program complex [14].

ACKNOWLEDGMENTS

The work was financially supported by the Russian Foundation for Basic Research (project no. 00-03-32567).

REFERENCES

1. Zvereva, I.A., Smirnov, Yu.E., Vagapov, D.A., and Choynet, J., *Zh. Obshch. Khim.*, 2000, vol. 70, no. 12, pp. 1957–1962.
2. Wells, A.F., *Structural Inorganic Chemistry*, Oxford: Clarendon, 1986, 5th ed.
3. Zvereva, I., Zueva, L., and Choynet, J., *J. Mater. Sci.*, 1995, vol. 30, no. 12, pp. 3598–3602.
4. Oudalov, Yu.P., Daoudi, A., Jourbort, J.C., Le Flem, G., and Hagenmuller, P., *Bull. Soc. Chim. Fr.*, 1970, vol. 10, no. 10, pp. 3408–3411.
5. Shannon, R.D., Oswald, R.A., Parise, J.B., Chai, B.H.T., Byszewski, P., Pajczkowska, A., and Sobolevski, R., *J. Solid State Chem.*, 1992, vol. 98, no. 1, pp. 90–98.
6. Smirnov, Yu.E. and Zvereva, I.A., *Vestnik Sankt-Peterb. Gos. Univ., Ser. 4: Khim.*, 1997, issue 4, no. 25, pp. 83–91.
7. Shannon, R.D., *Acta Crystallogr., Sect. A*, 1976, vol. 32, no. 5, pp. 751–766.
8. Ivernova, V.I. and Katsnel'son, A.A., *Blizhnii poryadok v tverdykh rastvorakh* (Short-Range Order in Solid Solutions), Moscow: Nauka, 1977.
9. Zvereva, I., Smirnov, Yu., and Choynet, J., *J. Mater. Chem. Phys.*, 1999, vol. 60, no. 1, pp. 63–69.
10. Smirnov, Yu.E. and Zvereva, I.A., *Zh. Obshch. Khim.*, 1996, vol. 66, no. 12, pp. 1971–1976.
11. Smirnov, Yu., Zvereva, I., and Choynet, J., *J. Solid State Chem.*, 1997, vol. 134, no. 1, pp. 132–137.
12. Tezuka, K., Hinatsu, Y., Mazaki, N., and Saeki, M., *J. Solid State Chem.*, 1998, vol. 138, no. 2, pp. 342–346.
13. Rietveld, H., *Appl. Crystallogr.*, 1969, vol. 2, no. 1, pp. 65–71.
14. Akselrud, L.G., Grun, Yu.M., Zavalii, P.Yu., Pechsky, V.K., and Fundamentsky, V.S., *CSD—Universal Program for Single Crystal AND/OR POWDER Structure Data Treatment. Collected Abstracts of XII European Crystallographic Meeting*, Moscow, 1989, vol. 3, p. 155.